

Size dependent phase stability of carbon nanoparticles: Nanodiamond versus fullerenes

A. S. Barnard,^{a)} S. P. Russo,^{b)} and I. K. Snook^{c)}

Department of Applied Physics, Royal Melbourne Institute of Technology University, GPO Box 2476V Melbourne, 3001, Australia

(Received 6 August 2002; accepted 19 December 2002)

Over the past 15 years, a number of studies have reported findings comparing the relative stability of diamond and graphite, at the nanoscale. In light of more recent experimental and theoretical results concerning the transformation of nanodiamonds into carbon-onions, it is considered important to extend this body of work to included fullerenes. Presented here is a study of the phase stability of carbon nanoparticles, with particular attention given to the relative stability of nanodiamonds and fullerenes. The structural energies have been calculated using density functional theory within the generalized gradient approximation using the Vienna *ab initio* simulation package, and used to determine the standard heat of formation for respective carbon phases as a function of the number of carbon atoms. Our results show that in contrast to previously reported studies, nanodiamond is not necessarily the stable phase at the nanoscale, but instead occupies a “window” of stability between ~ 1.9 and ~ 5.2 nm. © 2003 American Institute of Physics.
[DOI: 10.1063/1.1545450]

I. INTRODUCTION

For decades, it was known that graphite was the stable form of carbon at atmospheric pressures and that diamond, while harder, denser, and more durable, was merely metastable. With the discovery of buckminsterfullerene in 1980 the door was opened for a new era in carbon science, and scientists were introduced to a new carbon allotrope. Buckminsterfullerene and the extensive family of fullerenes (while not a true graphitic phase), share many structural characteristics with graphite such as sp^2 hybridization and six membered rings. The question of the mechanism of formation of fullerenes is currently hotly debated by fullerene research groups. It is agreed however, that the relative phase stability of graphite and fullerenes can be attributed to size dependence, and although the graphene-like structure of fullerenes is strained due to the curvature of the surface (and graphite is not), it is this strain that causes fullerenes to be more stable than other forms of sp^2 carbon at the nanoscale.¹

Recent interest in nanocrystalline diamond has prompted a number of researchers to re-examine the phase stability of diamond in the new nanosize regime. The transformation of nanodiamond to carbon-onions has been observed experimentally^{2–4} with a transformation temperature that is dependent on the size of the particle, and has been modeled theoretically^{5–9} at various levels of sophistication. Similarly, the reverse transformation of carbon-onions to nanocrystalline diamond has also been observed experimentally,^{10–14} and modeled¹⁵ by means of atomic-scale computer simulations.

The experimental discovery that nanodiamonds trans-

form to carbon-onions, and vice versa, appear to be contradictory to theoretical work compiled regarding carbon phase stability.^{5,16–22} Badziag *et al.* suggested that small hydrogenated nanodiamonds may be more stable than graphite, and Hwang *et al.* outlined a chemical potential model¹⁹ and a charged cluster model²⁰ to describe the relative stability of small diamond and graphite clusters in their study of low pressure diamond synthesis. Winter *et al.*⁶ also outlined a method for investigating carbon particle phase stability based on the heat of formation of graphene sheets and hydrogenated nanodiamonds. Most recently, Jiang *et al.*²² have calculated the size dependence of the diamond-graphite transition, using the Clausius–Clapeyron equation.

All of the above-mentioned methods predict nanodiamond to be the stable phase of carbon in the range less than about 6 nm. The present study represents an extension of this body of work, offering complementary findings regarding the phase stability of dehydrogenated nanodiamond particles. By treating only dehydrogenated nanodiamonds a direct comparison with fullerenes has been made possible.

Formation energy. The method of estimating the phase stability of nanoparticles used here is to determine the heat of formation, as a function of particle size. This technique was outlined by Winter and Ree,⁵ and is described in the following.²³ The atomic heat of formation of graphite ($\Delta H_f^o(G)$) and diamond ($\Delta H_f^o(D)$) clusters is expressed in terms of the C–C bond energy E_{CC} , the C–H bond energy E_{CH} , and dangling bond energy E_{DB} , such that

$$\Delta H_f^o(G) = \frac{1}{2}(3N_C - N_H)E_{CC}^G + N_H E_{CH}^G + N_C \Delta H_f^o(C) + N_H \Delta H_f^o(H) + \frac{1}{2}N_C E_{CC}^{vdw}, \quad (1)$$

$$\Delta H_f^o(D) = \frac{1}{2}(4N_C - N_{DB})E_{CC}^D + N_{DB} E_{DB}^D + N_C \Delta H_f^o(C) + N_{DB} \Delta H_f^o(DB), \quad (2)$$

^{a)}Electronic mail: amanda.barnard@rmit.edu.au

^{b)}Electronic mail: salvy.russo@rmit.edu.au

^{c)}Electronic mail: ian.snook@rmit.edu.au

where N_C is the number of carbon atoms, N_{DB} is the number of dangling bonds on the surface of the particle, N_H is the number of terminating hydrogen atoms, $\Delta H_f^o(C)$ is the standard heat of formation of carbon at 298.15 K, $\Delta H_f^o(H)$ is the standard heat of formation of hydrogen, and E_{CC}^{vdw} is the van der Waals attraction between graphite sheets. A dehydrogenated surface has been used for nanocrystalline diamond (see Eq. (2)), as the main intention here is to compare diamond with fullerenes, which do not have a hydrogenated surface. Dividing by N_C gives a heat of formation that is linear dependent upon the number of surface bonds per carbon atom N_H/N_C or N_{DB}/N_C :

$$\frac{\Delta H_f^o(G)}{N_C} = \frac{3}{2}E_{CC}^G + \frac{N_H}{N_C} \left(E_{CH}^G - \frac{1}{2}E_{CC}^G + \Delta H_f^o(H) \right) + \Delta H_f^o(C) + \frac{1}{2}E_{CC}^{vdw}, \quad (3)$$

$$\frac{\Delta H_f^o(D)}{N_C} = 2E_{CC}^D + \frac{N_{DB}}{N_C} \left(E_{DB}^D - \frac{1}{2}E_{CC}^D + \Delta H_f^o(DB) \right) + \Delta H_f^o(C). \quad (4)$$

We note that the various bond energies E_{CC} , E_{CH} , and E_{DB} are calculated at 0 K using Density Functional Theory (DFT) while $\Delta H_f^o(C)$ and $\Delta H_f^o(H)$ are determined at 298.15 K, but it has been assumed in this model that the corrections required due to this are small, and have therefore been ignored in this treatment. In their paper, Winter *et al.* assume sp^2 carbon to be three-fold coordinated, and the number of hydrogen terminations N_H refers to the edges of the graphene sheets, not to the surfaces.

In this present study this treatment has been extended to include fullerenes. In the case of fullerenes we know that each C atom is sp^2 hybridized like graphite however, Eq. (3) requires modification. First, fullerenes do not have interlayer attraction, so $E_{CC}^{vdw}=0$; and there are no hydrogen terminations or dangling edge bonds, so the N_H/N_C term is also zero, leaving:

$$\frac{\Delta H_f^o(F)}{N_C} = \frac{3}{2}E_{CC}^F + \Delta H_f^o(C). \quad (5)$$

However, this states that the atomic heat of formation for fullerenes $\Delta H_f^o(F)/N_C$ is a constant, and it does not account for the main difference between fullerenes and graphene sheets—the strain. Therefore, it is necessary to add a term for the strain energy (E_{strain}^F) that vanishes in the graphene limit.

Molecular calculations have shown that the predictions of continuum elasticity theory persist in the limit of radii < 1 nm.^{24,25} The continuum treatment used here to describe the strain energy of a fullerene assumes that there are only two in-plane elastic constants, and that the sheet is homogeneous and elastically isotropic. Hence, ignoring higher order effects such as torsional bending, the deformation energy consists of stretching (first-order) and bending (second-order) terms. In fullerenes, the stretching term is the cohesive energy of the carbon atoms, and the bending term provides the strain energy associated with curvature of the spherical structure.

$$E = E_{bend} + E_{stretch} = E_{strain} + E_{cohesive}. \quad (6)$$

Making the assumption that, for the general case, the strain in an elastic sphere can be modeled by considering the bending and stretching of a suitable elastic sheet, the bending energy (E_{strain}) per unit area (A) is given in terms of the sheet thickness (h), by

$$\frac{E_{strain}}{A} = \frac{\kappa}{2} \int_{-h/2}^{+h/2} dz \frac{z^2}{R^2} = \frac{\kappa h^3}{24R^2}, \quad (7)$$

where κ is the bending modulus of the sheet, and R is the radius of curvature. The strain energy per carbon atom is therefore:

$$\frac{E_{strain}}{N_C} = \frac{A \kappa h^3}{N_C 24R^2}. \quad (8)$$

For a fullerene, if we assume a spherical model, then R is also equal to the mean radius, $A = 4\pi R^2$, and $N_C = 4\pi R^2 \rho$. We have also assumed here that the number density ρ is a constant. This results in an expression for the strain energy per carbon atom, which is linearly dependent on the inverse square of the curvature of the structure:

$$\frac{E_{strain}}{N_C} = \left(\frac{\kappa h^3}{\rho 24} \right) \frac{1}{R^2} = E_{strain}^F \frac{1}{R^2}. \quad (9)$$

Note that the coefficient is scaling invariant, and that the strain energy E_{strain}^F is a constant. This is a suitable definition for use here as E_{strain}^F may be obtained by fitting the calculated energy to the inverse of the square of the fullerene curvature. Therefore, including this term in Eq. (1), the heat of formation for a fullerene is now given by

$$\frac{\Delta H_f^o(F)}{N_C} = \frac{3}{2}E_{CC}^F + \Delta H_f^o(C) + \frac{E_{strain}^F}{R^2}. \quad (10)$$

II. DISCUSSION

The nanodiamond and fullerene structures were relaxed using the Vienna Ab initio Simulation Package (VASP).^{26,27} We used ultrasoft, gradient corrected Vanderbilt type pseudopotentials²⁸ as supplied by Kresse and Hafner,²⁹ and the valence orbitals are expanded on a plane-wave basis up to a kinetic energy cutoff of 290.00 eV. The crystal relaxations were performed in the framework of DFT within the generalized-gradient approximation, with the exchange-correlation functional of Perdew and Wang (PW91).³⁰ Using this method, the calculated lattice parameter for bulk diamond of 3.561 Å, the sp^3 bond length of 1.541 Å, the band gap E_g of 5.46 eV are all in excellent agreement with the experimental values of 3.566 Å,³¹ 1.544 Å,³¹ and 5.48 eV³² respectively. Hence the same critical parameters were used in the study of the diamond nanocrystals.

In order to fully relax the structures, both the ions and supercell volume were relaxed. Each ionic step consisted of a minimum of three electronic steps (and a maximum of sixty electronic steps), followed by calculation of the Hellmann–Feynman forces. Thus, both the symmetry and the lattice parameter of the nanocrystals were free to alter, resulting in expansions or contractions of the entire structures. The relax-

ations were performed for a minimum of 20 ionic steps. A detailed description of this technique may be found in Ref. 33, and results for bulk diamond in Ref. 34.

A. Diamond, nanodiamond, and graphite

As a first step in this study, the heat of formation for graphite was considered, to offer a benchmark. The van der Waals attraction E_{CC}^{vdw} has been calculated by Guo,³⁵ using a graphite force field, to be 0.056 eV. Thus, using the experimental values for $\Delta H_f^o(C) = 7.432$ eV, $\Delta H_f^o(H) = 2.259$ eV, $E_{CH}^G = 3.507$ eV, and $E_{CC}^G = 4.917$ eV, the atomic heat of formation for graphite $\Delta H_f^o(G)/N_C$ was determined as a function of N_H/N_C as given in Eq. (11). As the experimental values were used for graphite it is reasonable to assume that these results will be accurate,

$$\frac{\Delta H_f^o(G)}{N_C} = 14.836 \text{ eV} + \frac{N_H}{N_C} 3.308 \text{ eV}. \quad (11)$$

Next, the heat of formation of cleaved bulk diamond and relaxed nanodiamond were determined separately. Recognizing that $\Delta H_f^o(DB)$ is the dissociation energy of the C–C bond, Eq. (4) becomes

$$\frac{\Delta H_f^o(D)}{N_C} = 2E_{CC}^D + \frac{N_{DB}}{N_C} \left(E_{DB}^D + \frac{1}{2} E_{CC}^D \right) + \Delta H_f^o(C). \quad (12)$$

Previously, the cohesive energy of bulk diamond and nanocrystalline diamond has been calculated,⁹ and found to be 7.39 and 7.71 eV, respectively. This equates to $E_{CC}^D = 3.695$ eV for bulk diamond and $E_{CC}^D = 3.855$ eV for nanodiamond. From the same linear fit to the spin polarization corrected energy per ion versus number of dangling bonds per ion used previously to determine the cohesive energy, the slopes give $E_{DB}^D = 1.433$ eV for bulk diamond and $E_{DB}^D = 1.619$ eV for nanodiamond. So, using the value of $\Delta H_f^o(C) = 7.432$ eV, with the values of E_{DB}^D and E_{CC}^D given for the above-mentioned bulk diamond and nanodiamond, the atomic heat of formation for diamond and nanodiamond $\Delta H_f^o(D)/N_C$ was determined as a function of N_{DB}/N_C as given in Eq. (13) for nanodiamond.

$$\frac{\Delta H_f^o(D)}{N_C} = 15.142 \text{ eV} + \frac{N_{DB}}{N_C} 3.547 \text{ eV}. \quad (13)$$

The atomic heats of formation for cleaved diamond (bulk diamond fragments), nanocrystalline diamond (relaxed nanodiamond crystals), and graphite were then plotted as a function of the number of carbon atoms. An empirical best fit was applied to the data sets, and the point of intersection determined, giving an estimate of the number of atoms at which a transition in phase stability occurs. In each case the equation of best fit was used, to which no physical meaning was assigned.

The results show that “cleaved” bulk diamond fragments are more stable than graphite for clusters less than 2345 atoms (approximately 2.4 nm in diameter), but are unstable compared to relaxed nanodiamonds of the same size. This is not surprising as it has been shown by many researchers that the structure of nanosized bulk diamond fragments

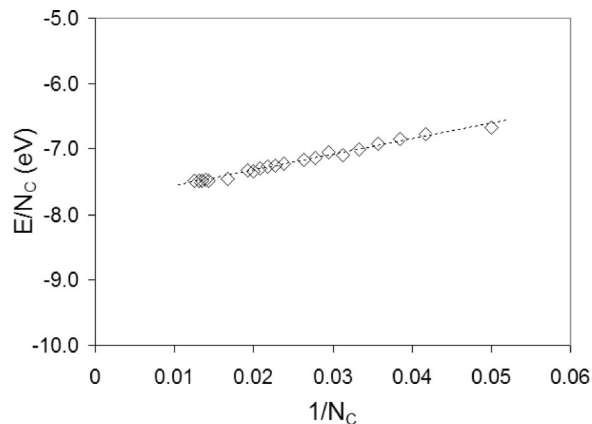


FIG. 1. Energy per ion for fullerenes C_{20} to C_{80} , showing the linear fit used to determine the cohesive energy and the strain energy.

alters upon relaxation. It was also found that relaxed nanodiamonds are more stable than graphite for crystals consisting of less than 24 398 atoms. This equates a crystal diameter of approximately 5.2 nm, beyond which graphite is the stable form of carbon, and diamond is metastable. This is lower than the PM3 results of Winter *et al.*,⁵ but is in agreement the model of Jiang *et al.*²² at 298.15 K.

B. Nanodiamonds and fullerenes

In order to determine the atomic heat of formation for fullerenes, it is first necessary to obtain the cohesive energy and the strain energy, both of which may be found by fitting Eq. (14) to the energy per ion versus $1/R^2$:

$$\frac{E}{N_C} = \left(\frac{\kappa h^3}{\rho 24} \right) \frac{1}{R^2} + \frac{E_{\text{cohesive}}}{N_C}, \quad (14)$$

where E is the total fullerene energy calculated explicitly with DFT, and $E_{\text{cohesive}} = (3/2)E_{CC}^F$. Here a problem arises in the estimation of the radius of curvature R for many of the fullerenes, as an atom may oppose the center of a ring on the other side of the fullerene. Therefore it is better to obtain R from the spherical approximation $N_C = 4\pi R^2 \rho$, where ρ was calculated easily from the C_{60} fullerene and found to be $0.37 N_C/\text{\AA}^2$. A number of the estimated radii were checked against the “measured” values of R (where possible), and found to be an excellent approximation.

Hence, the strain energy and cohesive energy obtained from the slope and intercept of the energy per ion versus $1/N_C$ were 5.19 and 7.81 eV, respectively (see Fig. 1). The calculated strain energy is slightly lower than the value of 6.56 eV of Hua *et al.*³⁶ using a quantum mechanical force field method (MSXX FF), but the cohesive energy is in excellent agreement with the cohesive energy of graphite at 298.15 K of 7.8 eV.³²

Using these results the atomic heat of formation was determined from Eq. (10), and plotted as a function of the number of carbon atoms. The C–C bond energy was extracted directly from the cohesive energy, as $E_{\text{cohesive}} = (3/2)E_{CC}^F$. Once again, a best fit was applied and the intersection with the nanodiamond results found. This intersection occurred at 1127 atoms, which is approximately equiva-

TABLE I. Size ranges of phase stability for small carbon clusters, including approximate diameters of cubic nanodiamond particles.

Stable allotrope	Carbon atoms (N_C)	Nanodiamond diameter (D)
Fullerenes	$0 < N_C < 1127$	$0 < D < \sim 1.9$ nm
Nanodiamond	$1127 < N_C < 24\,398$	~ 1.9 nm $< D < \sim 5.2$ nm
Graphite	$24\,398 < N_C < \infty$	~ 5.2 nm $< D < \infty$

lent to nanodiamond crystals of 1.9 nm in diameter. It is also interesting to note that the intersection point for graphite and fullerenes was 11 218 atoms. The relative ranges of stability of each carbon allotrope is given in Table I. In Table I the far right column refers to cubic nanodiamond particle sizes only, and that fullerenes or graphite particles with an equivalent number of atoms may vary in diameter.

III. CONCLUSIONS

It has been shown here, using a heat of formation model previously used successfully by Winter *et al.*,⁵ that nanocrystalline diamond is not necessarily the stable form of carbon at the nanoscale. Instead, fullerenes are the most stable form of carbon for small clusters, resulting in a “window” of stability for nanodiamond, in the range of approximately 1.9–5.2 nm in (cubic) diameter, beyond which graphite is most stable. In all but this range from ~ 1127 atoms to ~ 24398 atoms, diamond is metastable.

These results are considered to be very useful in explaining the transition of nanocrystalline diamond to carbon onions, during *ab initio* relaxations. The upper limit of fullerene stability falls above the upper limit of the capability of current computers, using *ab initio* methods, thus in the size range of all recent *ab initio*⁹ or semiempirical^{5–8} studies, fullerenes are the most stable phase of carbon.

Our results are further supported by a number of other experimental and theoretical investigations. Recently nanocrystalline diamond has been obtained directly from carbon nanotubes at high pressure;³⁷ and the theoretical relaxation of carbon multiwalled nanotubes has been performed using the empirical many-body potential energy functional and (canonical) molecular dynamics at 1 K^{38,39} by Erkoç *et al.*, showing the beginning of their transformation into what is best described as ta–C nanorods, in line with experimental observations.⁴⁰

ACKNOWLEDGMENTS

We would like to thank the Victorian Partnership for Advanced Computing and the Australian Partnership for Advanced Computing supercomputer center for their ongoing support over the course of this project.

- ¹P. R. C. Kent, M. D. Towler, R. J. Needs, and G. Rajagopal, Phys. Rev. B **62**, 15394 (2000).
- ²V. L. Kuznetsov, A. L. Chuvilin, Y. V. Butenko, I. Y. Mal’Kov, and V. M. Titov, Chem. Phys. Lett. **209**, 72 (1994).
- ³V. L. Kuznetsov, I. L. Zilberberg, Y. V. Butenko, A. L. Chuvilin, and B. Seagall, J. Appl. Phys. **86**, 863 (1999).
- ⁴S. Tomita, T. Sakurai, H. Ohta, M. Fujii, and S. Hayashi, J. Chem. Phys. **114**, 7477 (2001).
- ⁵N. W. Winter and F. H. Ree, J. Comput.-Aided Mater. Des. **5**, 279 (1998).
- ⁶F. H. Ree, N. W. Winter, J. N. Glosli, and J. A. Viecelli, Physica B **265**, 223 (1999).
- ⁷F. Fugaciu, H. Hermann, and G. Seifert, Phys. Rev. B **60**, 10711 (1999).
- ⁸H. Hermann, F. Fugaciu, and G. Seifert, Appl. Phys. Lett. **79**, 63 (2001).
- ⁹A. S. Barnard, S. P. Russo, and I. K. Snook, Philos. Mag. Lett. **83**, 1, 39 (2003).
- ¹⁰F. Banhart and P.M. Ajayan, Nature (London) **382**, 433 (1996).
- ¹¹F. Banhart, J. Appl. Phys. **81**, 3440 (1997).
- ¹²M. Zaiser and F. Banhart, Phys. Rev. Lett. **79**, 3680 (1997).
- ¹³Ph. Redlich, F. Banhart, Y. Lyutovich, and P. M. Ajayan, Carbon **36**, 561 (1998).
- ¹⁴M. Zaiser, Y. Lyutovich, and F. Banhart, Phys. Rev. B **62**, 3058 (2000).
- ¹⁵R. Astala, M. Kaukonen, G. Jungnickel, Th. Frauenheim, and R.M. Nieminen, Phys. Rev. B **63**, 081402 (2001).
- ¹⁶J. A. Nuth, Nature (London) **329**, 589 (1987).
- ¹⁷P. Badziag, W. S. Veowoerd, W. P. Ellis, and N. R. Greiner, Nature (London) **343**, 244 (1990).
- ¹⁸M. Y. Gamamik, Nanostruct. Mater. **7**, 651 (1996).
- ¹⁹N. M. Hwang, J. H. Hahn, and D. Y. Yoon, J. Cryst. Growth **160**, 87 (1996).
- ²⁰N. M. Hwang, J. H. Hahn, and D. Y. Yoon, J. Cryst. Growth **162**, 55 (1996).
- ²¹P. Keblinski, S. R. Phillpot, D. Wolf, and H. Gleiter, Nanostruct. Mater. **12**, 339 (1999).
- ²²Q. Jiang, J. C. Li, and G. Wilde, J. Phys.: Condens. Matter **12**, 5623 (2000).
- ²³Note that modifications have been made to the nomenclature, as this method is to be extended to describe more than one form of sp^2 carbon.
- ²⁴D. H. Robertson, D. W. Brenner, and J. W. Mintmire, Phys. Rev. B **45**, 12592 (1992).
- ²⁵J. P. Lu, Phys. Rev. Lett. **79**, 1297 (1997).
- ²⁶G. Kresse and J. Hafner, Phys. Rev. B **47**, 558 (1993).
- ²⁷G. Kresse and J. Hafner, Phys. Rev. B **54**, 11169 (1996).
- ²⁸D. Vanderbilt, Phys. Rev. B **41**, 7892 (1990).
- ²⁹G. Kresse and J. Hafner, J. Phys.: Condens. Matter **6**, 8245 (1994).
- ³⁰J. Perdew and Y. Wang, Phys. Rev. B **45**, 13244 (1992).
- ³¹H. J. McSkimin and P. Andreatch, J. Appl. Phys. **43**, 2944 (1972).
- ³²A. Mainwood, *Properties and Growth of Diamond*, edited by G. Davies (INSPEC, London, 1993), p. 3.
- ³³J. Furthmüller, J. Hafner, and G. Kresse, Phys. Rev. B **53**, 7334 (1996).
- ³⁴A. S. Barnard, S. P. Russo, and I. K. Snook, Philos. Mag. B **82**, 1767 (2002).
- ³⁵Y. Guo, Ph.D thesis, California Institute of Technology, 1992.
- ³⁶X. Hua, T. Çağın, J. Che, and W. A. Goddard III, Nanotechnology **11**, 85 (2000).
- ³⁷H. Yusa, Diamond Relat. Mater. **11**, 87 (2002).
- ³⁸S. Erkoç, Int. J. Mod. Phys. C **11**, 1247 (2000).
- ³⁹S. Erkoç and O. B. Malcioglu, Int. J. Mod. Phys. C **11**, 1247 (2000).
- ⁴⁰K. H. Chen, C. T. Wu, J. S. Hwang, C. Y. Wen, L. C. Chen, C. T. Wang, and K. J. Ma, J. Phys. Chem. Solids **62**, 1561 (2001).